Journal of Techniques, ISSN: 2708-8383, Vol. 6, No. 1, 2024, Pages 93-102
DOI: https://doi.org/10.51173/jt.v6i1.1418

JOURNAL OF TECHNIQUES

Journal homepage: http://journal.mtu.edu.iq

RESEARCH ARTICLE - MATERIAL SCIENCE (MISCELLANEOUS)

Optical Observations of Sputtered Au-nanostructures and Characterizations

Sabah Jameel Mezher[1*], Mohammed O. Dawood[1], Bahjat B. Kadhim[1]

[1]Department of Physics, College of Science, Mustansiriyah University, Baghdad, Iraq

[*] Corresponding author E-mail: sabah.jamil@uomustansiriyah.edu.iq

Article Info.

Article history:

Received
16 April 2023

Accepted
02 August 2023

Publishing
31 March 2024

Abstract

To develop novel optoelectronic devices, controlling and predetermined absorption is necessary. In the current work, the gold nano-islands were sputtered onto quartz surface substrates using a DC sputtering unit with an optimized chamber. The effects of the sputtering time (10, 15, and 20 seconds) on the characteristics of the golden layers deposited on quartz substrates were studied. Au nanofilms were investigated by XRD (X-ray diffraction), UV-Vis (ultraviolet-visible light) diffractometer, and AFM (atomic force microscopy) techniques. The thicknesses of the three films prepared at different sputtering times (10, 15, and 20 seconds) were calculated using the theoretical deposition formula method. The average layer thickness, and hence the size of the golden crystallites, rose from 6.8 to 13.6 nm when the sputtering period was increased. The X-ray spectra revealed a very distinctive peak at (111), indicating that the gold single crystal is fully oriented along [111] and the gold film has a pure crystalline FCC structure. When deposition times are lengthened, the color of the resulting films change from blue to green. Nano-films have shown important changes in their surface shape and roughness. The structural layer of Au's surface is remarkably semi-spherical, giving it a spherolitic and hummock-like appearance. Analyzing the UV-VIS spectra of the precipitated structures using Tauc's paradigm revealed the optical energy gap (non-zero Eg in the range of 2.36 to 2.38 eV) that is associated with the nanostructure's semiconducting properties. In addition, as the sputtering duration increases from 10 to 20 seconds, the wavelengths at which peak values of the surface plasmon resonance occur shift from 610 to 650 nm, and the widths of the peaks rise. The AFM images of the ultra-thin Au layers showed smooth surfaces whose roughness decreases from 1.82 to 0.673 nm with increasing sputtering time from 10 to 20 seconds. Solar cells can take advantage of the higher absorption in the blue spectrum region by using a set of depositing parameters and prescribed thicknesses. In addition, the formation of nano-islands can also be used as nucleation sites (seed layer) to promote the growth of various nanostructures to obtain a good aspect ratio and improve the performance of various optoelectronic devices and gas sensors.

Publisher: Middle Technical University

Keywords: Au Nanoparticles; DC-Sputtering; Optical Properties; XRD; AFM.

1. Introduction

The many fields and purposes that can be met by nanotechnology contribute to its ever-growing popularity [1-3]. Noble metal nanostructures, such as those made of Au or Ag, have been actively investigated for decades because of human demand for innovative properties of materials, in particular because of their stunning qualities in the visible spectrum [4-6]. At present, nanotechnology is a major factor in almost every field of study [7]. It has been widely adopted in the chemistry, engineering, and technology industries, and is even making its way into the medical and pharmaceutical fields [8]. This is due to its great stability, low size and density, high surface area-to-volume ratio, and high chemical reaction efficiency [5]. It was found that the electromagnetic model proposed by Drude in 1894 to explain the optical characteristics of metals agreed with experimental data from the deposited thin films [9,10]. Not only do nanostructures of noble metals have interesting catalytic and electrical properties, but they also have unique form-dependent optical qualities that have garnered major technological applications, and this is especially true for gold nanoparticles due to their plenty [11,12]. Considerably thin metal films have optical characteristics very different from those of bulk metals, and this difference cannot be explained by changes in the metal's nature [10, 13]. It was Garnett, in 1904, who proposed that the discontinuity form nature of quite thin films, which can consist of tiny aggregates and very tiny islands, could account for this variation in optical characteristics [10-14].

Metallic gold nanoparticles are employed as a catalyst seeds layer to promote the nucleation and produce 1D nanostructures of metal oxides like ZnO nanostructures. This catalyst seeds layer improves the characteristics of nanostructures utilized in applications such as chemical gas sensors and solar cells [15-17]. Previous research has revealed that the structure and size of gold nanoparticles affect their thermodynamic stability [18]. When gold nanoparticles' size is lowered, their melting temperature will drop dramatically [19][20]. However, the melting point scales with the dimensions of a material as its size drops toward the nanoscale level and approaches the atomic scale [10]. Gold nanofilm layers are used in a wide variety of modern electronic applications, including microelectronic and nanoelectronic systems (MEMS and NEMS) and chemical sensors [21-23]. Chemical and physical techniques, such as chemical vapor deposition (CVD), thermal evaporation, physical vapor deposition (PVD), direct current (DC) sputtering deposition, sol-gel deposition, pulsed laser ablation, and electrochemical precipitation, can all be used to produce Au nanostructures [24-27].

Nomenclature & Symbols			
Eg	Energ Gab	AFM	Atomic Force Microscopy
t	Sputtering Time	θ	Bragg's Diffraction Angle
hν	Photon Energy	α	Absorption Coefficient
β	Half-Width At Half-Maximum	ε	Strain
δ	Dislocation	K	Material Characteristic
D	Crystalline Size	RMS	Roughness
SPR	Surface Plasmon Resonance	I	Sputtered Current
d	Film Thickness	V	Applied Voltage

In this work, gold nano-islands were sputtered at various sputtering times (10, 15, 20 seconds) onto quartz substrates using the DC sputtering technique. It is important to study the change of optical, structural, and morphological properties of sputtered golden layers as a function of sputtering time and the relationship of this to the different mechanisms of movement of charge carriers. In addition, the study investigates the formation of these gold nano-islands as they transform from bulk material to nanoscale, and aims to understand the potential of utilizing the unique features of these nanofilms that could significantly impact the future manufacture of solar cells and enhance many optoelectronic devices.

2. Materials and Method

Soap and water were used to clean quartz substrates (1.5 x 2.5 cm²) before the substrates were sonicated in methanol and acetone for 10 minutes. After being washed with distilled water, the substrates were blown dry with nitrogen gas. An ion coater (3Targate Plasma Sputtering Coater MTI Corporation, shown in Fig. 1) was used for the sputtering of gold nanofilm layers on the quartz substrates. DC Ar plasma, 7.5 W of discharge power, 99.995 % pure gas 10, 15, and 20 seconds of sputtering time: these were the parameters for deposition.

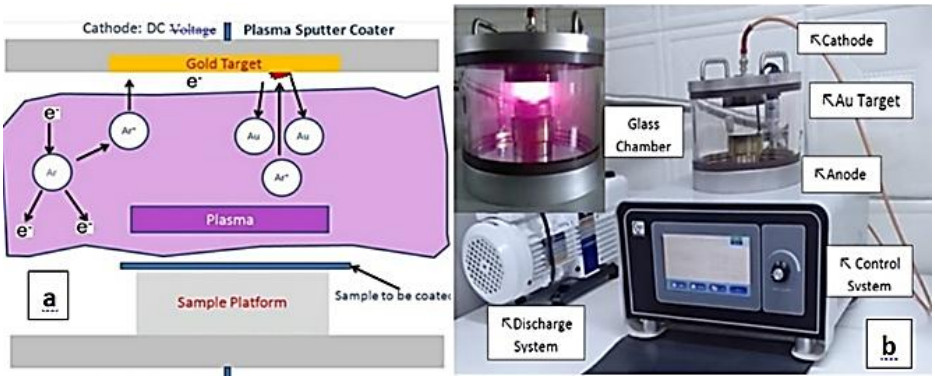

Fig. 1. a. Show the plasma process [28], b. Ion Coater sputtering system

The produced Au nanofilms' crystalline structures were examined using an X-ray diffractometer (X'Pert High Score PANalytical 021-44862778, Philips PW1730) that was set to 40 kV and 30 mA, with Cu Kα radiation (λ = 1.54056 ºA). UV-VIS spectrophotometer (BEL Engineering UV-M51 Single Beam Spectrophotometer of the wavelength range 200-1100nm) was used to examine the optical properties. Absorption coefficients were calculated from optical measurements and plugged into Tauc's equation [24], $\alpha(\nu) = A(h\nu - E_g)^x h\nu$, in which α (the absorption coefficient), E_g is the (optical band gap) of the substance, x specifies the (type of electron transition), and A (factor relies on the transition eventuality) and is assumed to remain consistent within the range of the optical frequency. In these nanolayers, indirect transition cannot be eliminated; therefore, x = 1/2 may be utilized in the equation. Following this, the E_g (Optical band gap width) was determined through linear extrapolation of plots $(\alpha h\upsilon)^{1/2}$ versus photon energy (hυ). Atomic force microscopy (AFM AA2000 / SPM) was used to investigate the deposited films' topography and morphology [29].

3. Results and Discussion

Sputter coating works by using a heavy gas to ionize metal target atoms like gold. Quartz substrates are placed into the coating unit, and then the ionization gas ejects gold particles from the target, which travel across the plasma and are deposited on the quartz substrates. In a low vacuum setting, a low voltage sputtering coater technology may deposit metal at rates of up to 1 nm/s (0.02 to 0.15 mbar). The sputtering coater method employed in this research had a deposition rate of 0.68 nm/s. The parameters for Au sputter deposition are shown in Table 1.

Table 1. Sputter coater settings for sputtering. (MTI Corporation)

Working pressure (mbar)	Base pressure (mbar)	Flow rate (sccm)	Current (mA)	Applied voltage (kV)
1.5 x 10-1	0.2×10^{-1}	150	4.0	1.0

An ion coater is a plasma sputter coater used to deposit metallic nanostructured layers, like Au or Ag. Different time sputtering (10, 15, and 20 seconds) was used to depose Au nanostructure films successfully using a DC sputtering system (3Targate Plasma Sputtering Cotter MTI Corporation). Because of its precision and dependability, this method can be utilized to manufacture a large variety of nanostructures and may be employed in the construction of a wide range of electronic devices, such as gas sensors and solar cells [30-32]. The plasma sputter process includes three main steps [33] (see Fig. 1):

- The sputtering chamber must be purged using Ar gas and the pressure must be reduced to 1.5×10^{-1} mbar to increase the intermolecular spacing between argon molecules.

- The cathode emits electrons when a high voltage of 1 kilovolt (kV) is supplied to it. Electrons, boosted by the electric field, smash into the argon molecules in the vacuum chamber. As the Ar plasma forms, a purple glare can be seen (Fig. 1-a).

Gold particles are deposited on the substrates after energetic Ar ions gain energy in an electric field and smash into a gold target (Fig. 1-b).

3.1. Dependence of film thickness on sputtering time

The thickness d of the deposited thin films is influenced by many factors, including the type of the target material, applied voltage V, sputtered current I, and deposition time t. A close description of the connection between these variables can be observed in the following theoretical deposition formula [29, 13]:

$$d = KIVt \quad (1)$$

To be more precise, the material characteristic, K, is 0.17 for gold in Ar gas. As sputtering time increases, the amount of gold particles removed from the target increases. This leads to the expected increase in film thickness, as shown in Fig. 2. These results are consistent with the findings of the researchers Abdulqader et al. [29].

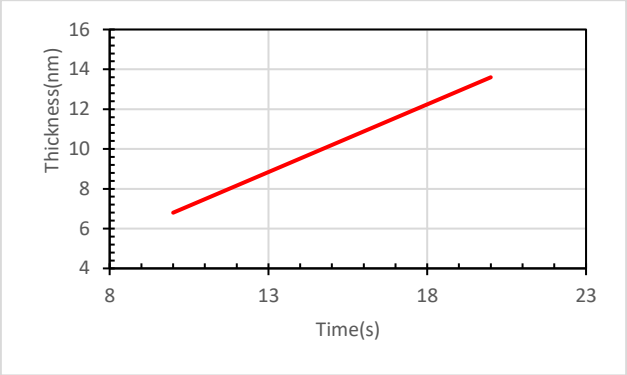

Fig. 2. Thickness of gold film vs. Sputtering time (10, 15, and 20 seconds)

Table 2 displays the results of applying the empirical equation (eq. 1) to calculate the thickness of the three films prepared at different sputtering times. We could not measure the thickness of the deposited films using the SEM test, as the films burned inside the test device due to their very small thickness.

Table 2. Thicknesses of 3 samples for (10, 15, and 20 seconds) sputtering time

Sputtering Time (s)	**10**	**15**	**20**
Thickness (nm) by Empirical Method	6.8	10.2	13.6

3.2. X-Ray Diffraction

X-ray diffraction (XRD) is a non-destructive analytic technique that can disclose crucial details about the lattice structure of a crystalline substance, such as the dimensions of the unit cell, chemical characteristics, bond angles, and crystallographic structure of both synthetic and natural substances. The XRD method relies on the idea of constructive interference between X-rays and the specimen, which can only be achieved with a crystalline specimen. Bragg's law, which describes the interaction responsible for the production of constructive interference when x-rays are incident on a sample, connects the wavelength of the incident radiations to the diffraction angle and lattice spacing [34][35]. Using an X-ray diffractometer system, we analyzed the crystal structure of Au that had been sprayed onto quartz surfaces (for 20 s sputtering time). Fig. 3 depicts the diffraction peaks for reflection from the planes (111), (200), and (311) at 2θ = 38.184º, 44.392º, and 77.547º. The X-ray spectra revealed a very distinct peak at (111), indicating that the gold single crystal is fully oriented along [111] and the gold film has a pure crystalline fcc structure that matches card number 00-004-0784 [36, 37].

To calculate the crystalline size (D nm) of the Au nanostructure, Scherrer's equation was used as follows [38][39]:

$$D = \frac{0.9\lambda}{\beta\cos\theta} \quad (2)$$

in which λ is the wavelength, θ is Bragg's diffraction angle, and β is the FWHM (half-width at half maximum). Table 3 displays the outcomes of an XRD investigation performed on an Au nanostructure.

The microstrain Ɛ for the Au film is determined by the formula:

$$\varepsilon = \frac{\beta\cos\theta}{4} \quad (3)$$

while the density of dislocation δ that indicates a crystal imperfection related to the distortion of the lattice is determined by the equation:

$$\delta = \frac{1}{D^2} \quad (4)$$

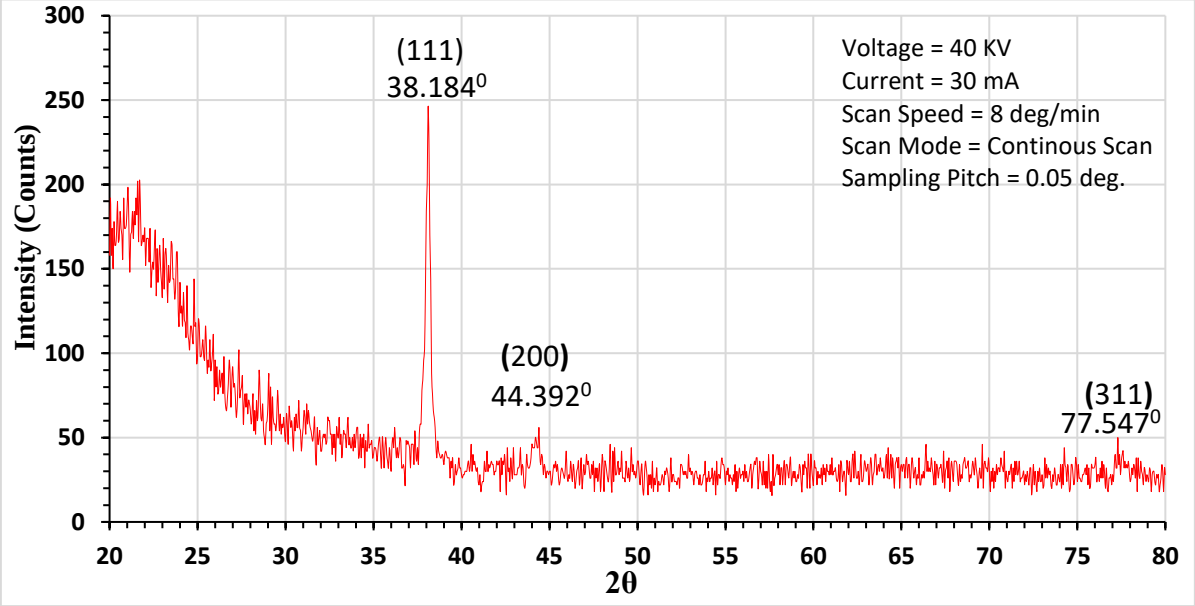

Fig. 3. The X-ray pattern of a gold film sputtered onto a quartz surface

Table 3. Structural parameters for Au nanostructure layer

(hkl)	2θ (deg)	Beta(rad.)	Crystallite size D (nm)	(ε) Strain×10^{-4} (lines^2/m^4)	(δ) Dislocation ×10^{14} (1/m^2)	d(⁰A) Exp.	d(⁰A) Theor.
(111)	38.184	0.0040	34.6	7.9	8.4	2.30	2.36
(200)	44.392	0.0052	26.9	9.2	13.8	1.99	2.04
(311)	77.547	0.0047	29.5	2.5	11.4	1.20	1.23

As crystals are regrown close to their surfaces, the lattice parameters swerve from their typical values. This deflection is particularly noteworthy for nano-crystal structures because of their large surface area to core ratio [40, 41]. It is observed that the produced samples have varying lattice parameters depending on sputtering time. Specifically, when the deposition period increases, the average layer thickness and size of the gold crystallites both increase with sputtering time, matching the findings of V. Vorak et al. [42].

3.3. Effect of sample thickness on obtaining accurate and reliable XRD data

The lattice parameters of metallic nanostructures formed as thin nanofilms by a physical deposition technique are not material invariant but greatly rely on the nanolayer thickness, as shown previously in other work [43, 44]. The dependence shows that the lattice parameter declines monotonically with layer thickness. Relaxation of internal stress during gold cluster formation explains this phenomenon [45]. Only samples thicker than 10 nm can have their lattice parameter calculated for thin metal films (here gold) [30]. To find out how a decrease in lattice parameters affects the density of gold structures, it is necessary to measure the effective thickness and mass of deposited structures and calculate the effective density by a standard method. The density rises as the layer gets thicker; at around 90 nm, it attains the density of bulk gold. The increased fraction of free volume in gold nanoclusters is likely to be blamed for the lower density of thinner structures. As has been reported elsewhere, X-ray diffraction experiments revealed that the lattice parameter decreased monotonically with increasing thickness. Measurements of the effective weight and thickness of the formed nanostructures show that the density of the deposited Au increases as the structure thickness increases [30]. At thicknesses of layers greater than 90 nm, the bulk value is attained. As the clusters become larger, the ratio of free volume decreases while the gold density increases [46]. Previous research has shown that gold layers thicker than 100 nm formed on glass substrates have a uniform density with a mean value of 19.3 g cm^{-3} typical of bulk material [30, 40].

3.4. UV-VIS Characteristics

Group 11 of the periodic table is where you'll find gold and the other transition metals. In addition to being resistant to most acids, including nitric acid and hydrochloric acid, gold is also regarded as a noble metal because of this property [43-45]. Photographs of the nanostructured gold samples' surfaces after being sputtered for different durations are shown in Fig. 4. Increasing the sputtering time resulted in darker precipitated samples, and we also observed a little change in color from blue to green; this was probably because the darker color was related to the thickness of the gold structure, as seen in the photographs. As can be seen from these observations, the gold layer thickens with continued sputtering, going from 6.8 nm at 10 seconds to 10.2 nm for 15 seconds to 13.6 nm following 20 seconds [42, 45].

UV/Vis optical spectra of ultrathin Au nanofilms are structure-dependent [46-48]. Depending on the medium, surface structure, particle size, and form, the localized absorption characteristic of Au films can change significantly [49]. The optical absorption spectra of a gold nanostructure layer sputtering onto quartz substrate surfaces for 10, 15, and 20 seconds are shown in Fig. 5 using data from UV-VIS spectrophotometer examinations. The absorbance of the gold nanocrystalline films rises as the sputtering duration increases, as shown in the graph (and hence, with increasing thickness). The spectrum measurements show a minimum absorption at roughly 500 nm, shifting slightly to red as the nanofilms became thicker [30].

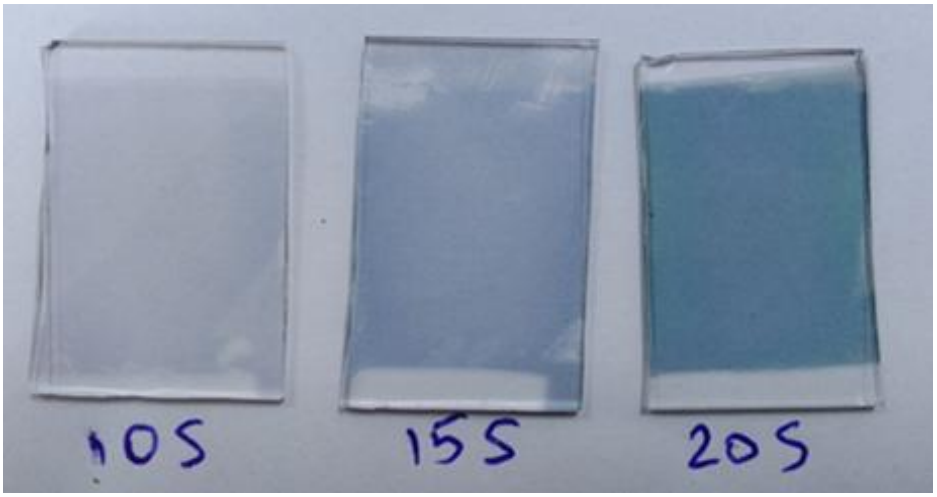

Fig. 4. Samples photographed of quartz with gold structures at various times

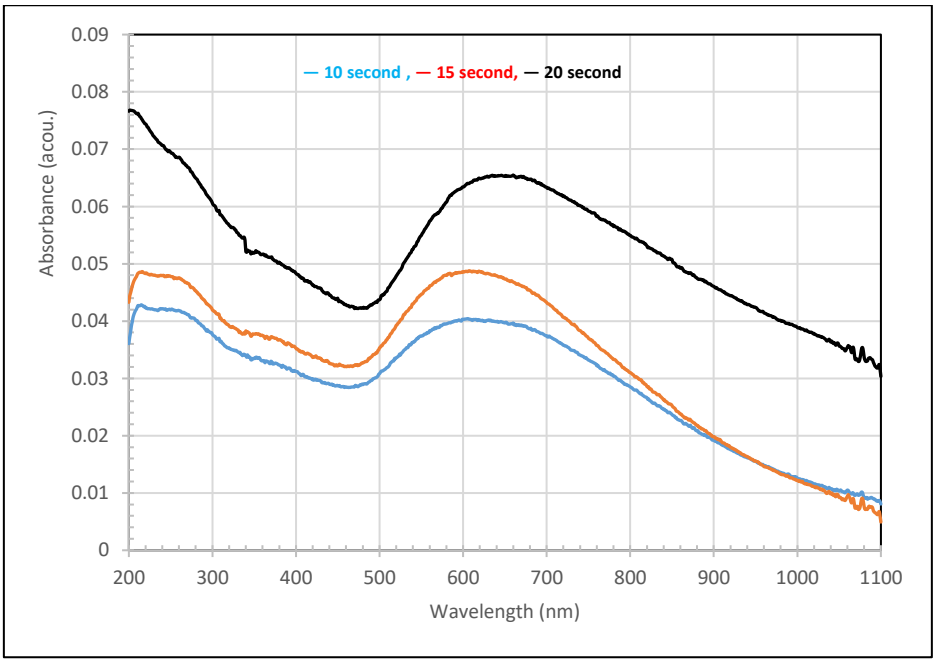

Fig. 5. Absorption changes in the Au nanofilms as a function of wavelength (nm)

At the interface of dielectric/metal, free electrons interact with light, resulting in the formation of surface plasmons (SPs). Under particular conditions, the excitation of the SPs results from the oscillation of the free electrons at the metallic surface in resonance with the incident light wave and will either be propagated along the interface or confined to the metallic particles [50]. It has been shown that particle shape, size, and environment all affect the position and width of the SPR resonant peak [4,51,52]. The absorption peak moves to longer wavelengths with increasing sputtering duration, likely due to the interlinked and mutually interactive structure of gold nanoparticles, which may be accountable for this observation. According to experimental reports, with an increase in the nominal thickness of the film, the wavelength of the plasmon resonance shifts to red [53, 54]. Many researchers have correlated this redshift to variations in the aspect ratio, or dimensions, of the nano-islands [4, 55]. A high absorbance value for the sputtered structure is indicative of a discrete gold islands formation. It is well known that as the size of a spherical gold nanoparticle grows, the wavelength of the single peak attributable to the localized plasmon shifts to the longer side (redshifts) and extends in width as the particle size grows [8]. Higher absorption was observed at longer wavelengths, which may be due to the effect of surface plasmon resonance [56]. Inhomogeneous and discontinuous layers composed of nanometer-sized metallic clusters that are 6.8 to 13.6 nm thick reveal the absorption in the visible region. This phenomenon is attributed to the SPR in the metallic islands, where the surface plasmon peak is shifted from 610 to 650 nm at 10 and 20 seconds of sputtering time, respectively. It is common knowledge that the optical absorbance of gold nano-island films is a function of the density of the gold islands [57]. As the density of the islands rises, the absorption band caused by the particles' bounded plasma resonance shifts to longer wavelengths. With increasing cluster size (film thickness), the absorption band broadens due to a more even distribution of particle sizes, and a redshift also occurs with increasing cluster size [30]. In any case, two unique peaks appear whenever gold nanoparticles are sputtered onto a quartz substrate. The position and width of each of these peaks are influenced by the sputtering duration, which is compatible with Priyabrata Pattnaik's research work [29]. The optical technique known as surface plasmon resonance (SPR) is used to study the refractive index of adsorbing metal layers' surfaces. An extremely small amount of absorbed light energy at an extremely narrow angle might decrease the reflected light through interactions with non-specific electrons in the metallic layer (plasmonic). The SPR technology is based on the notion that photons can be transformed into surface plasmons by exciting the plasmons on the surface of a metal nanofilm using light of a specific wavelength (the wavelength being determined by the adsorbent's refractive index). Two

absorption peaks are observed for the two deposited gold nanofilms due to plasmonic transformations and innerband interactions (10 and 15-second sputtering time). The long-wavelength area is where the plasmonic peaks reside (redshift) [30, 42]. UV-Vis spectra were analyzed using the famous Tauc's model and measuring the optical band gap (E_g) of sputtered specimens for different sputtering times. Fig. 6 graphically displays this correlation. Sputtered structures with a sputtering time of less than 20 seconds show a non-zero optical energy gap (see Figure). To properly comprehend the behavior of ultra-thin metal nanostructures (< 20 nm), it is necessary to consider both the quantum-size and surface-size effects. This quantum-size effect in small structures leads to a non-zero optical energy gap (Eg) and the semiconducting behavior of the gold nanostructure. A non-zero band gap indicates semi-conducting properties of the sputtered gold nanostructures. The valence band and the conduction band overlap in the metal block (gold block), while in semiconductors there is a forbidden band gap that separates the valence band and the conduction band. The presence of a non-zero band gap in the sputtered gold structures indicates that these structures possess semiconductor properties [24]. This effect has been observed here. The influence of quantum confinement is especially noticeable in the blue part of the spectrum, in which peaks with low nanoparticle dimensions may be observed in Fig. 5, where the system of quasi-static or the zone of intrinsic volume is famous. When compared to prior investigations on the subject of gold nano-islands precipitating via thermal evaporation, redshift's findings were consistent [38].

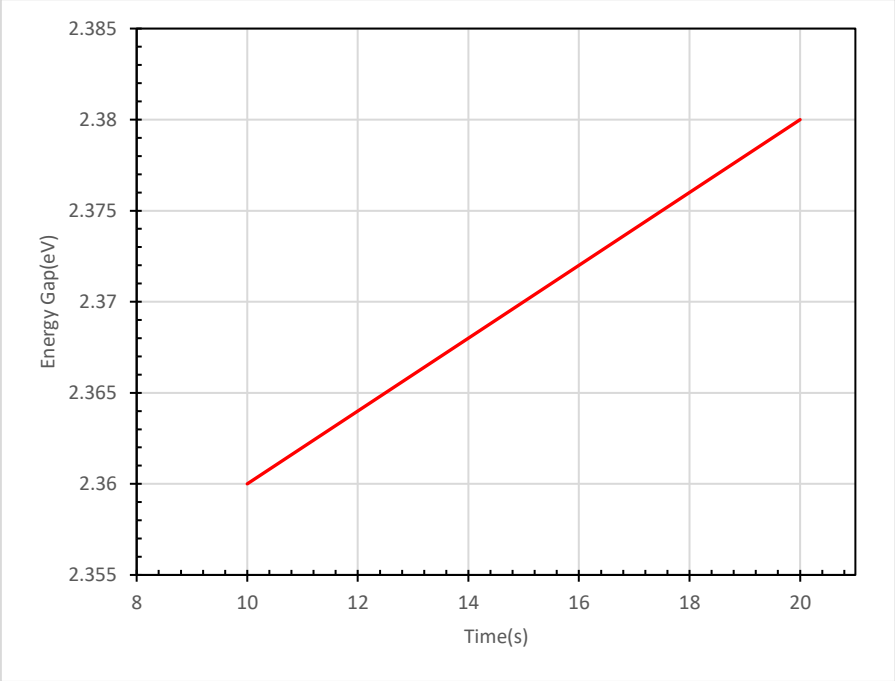

Fig. 6. Variation in optical energy gap (eV) as a function of gold nanostructure sputtering time(s)

3.5. AFM Characteristics

The topography of the film's surface can be studied with great detail using an atomic force microscope (AFM). Using an air-operated AFM, the surface morphology and roughness of Au films created by DC sputtering on quartz substrates were analyzed. Fig. 7 shows images captured by an atomic force microscope which reveal the surface morphology of the gold layer after 10, 15, and 20 seconds of sputtering (Figs. 7-a, b, and c, respectively). Fig. 7 shows that the surface configuration of the as-sputtered nanostructures does not rely noticeably on the sputter times. The structural layer of the Au surface is remarkably semi-spherical, giving it a spherolytic and hummock-like appearance. The layered growth stage is related to the monotonic decline of surface roughness (in the range 1.82-0.673 nm) with deposition time, and it was found that the diameter of the nanoparticles is about (58.84 to 49.77 nm) nm on average. When comparing the average particle size obtained from AFM images to the crystallite sizes obtained from the X-ray pattern for gold films, there is a high level of consistency in the growing mode (see Table 4). The stage of layer growth is related to the monotonic decline in surface roughness with deposition time. During the earliest stages of metal film forming, the layer is formed from isolated islands. After that, during subsequent deposition, linkages are formed between clusters, and the resulting layers are uniform and homogeneous. A thicker layer has grown during the sputtering process as seen by a decrease in the surface roughness of the substrates.

Table 4. Measurements of AFM test for DC-sputtered Au nanofilms, including their mean particle size, roughness, and root-mean-squared roughness

Sample No.	Sputtering Time(s)	AU Thickness (nm)	Average Roughness(nm)	RMS Roughness(nm)	Average Diameter (nm)
S1	10	6.8	1.82	2.49	58.84
S2	15	10.2	1.18	1.52	57.16
S3	20	13.6	0.673	1.03	49.77

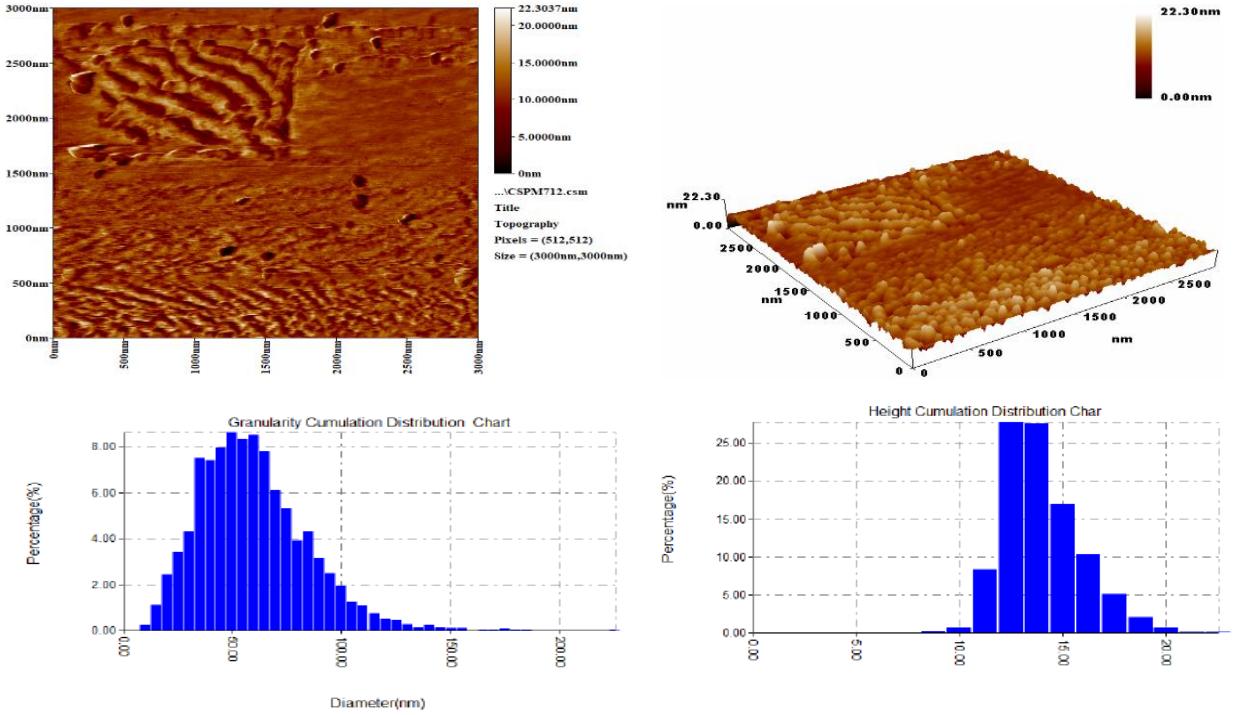

Fig. 7. a. AFM image of Au nanofilm layer deposited at 10-second sputtering time

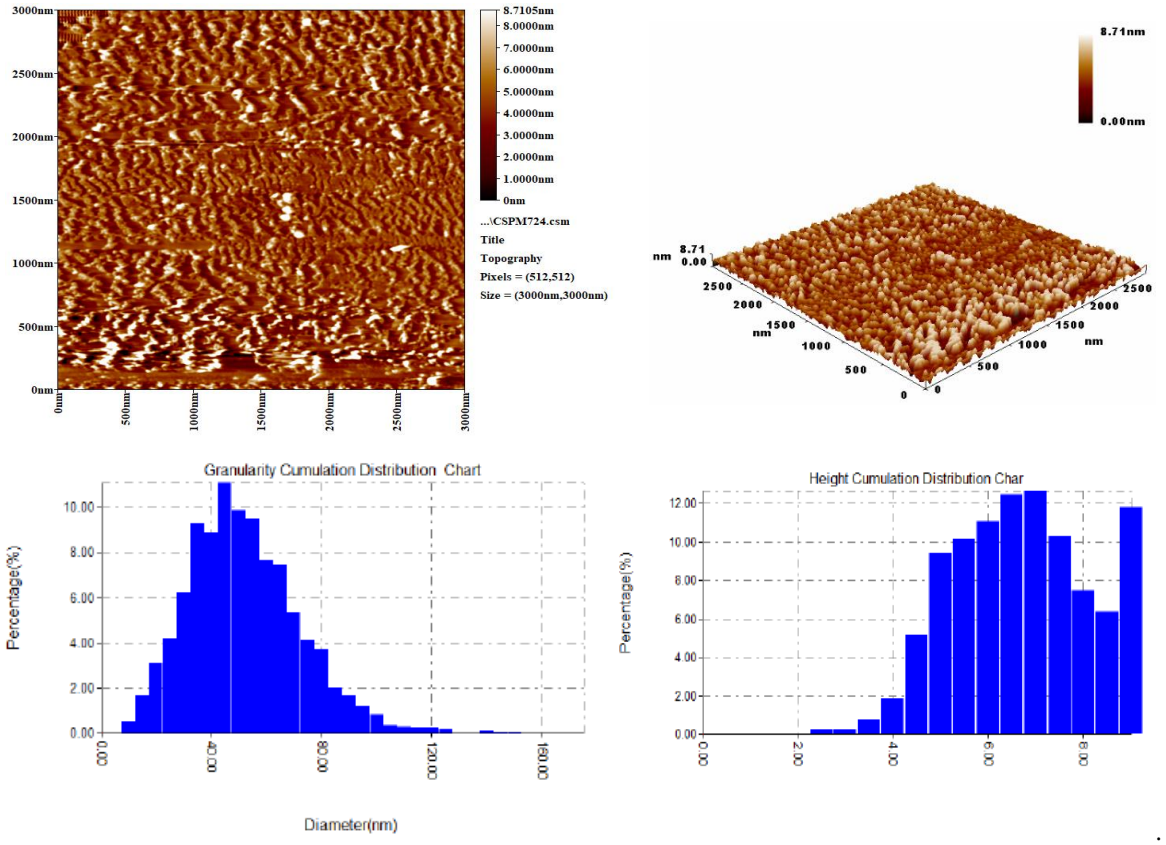

Fig. 7. b. AFM image of Au nanofilm layer deposited at a 15-second sputtering time

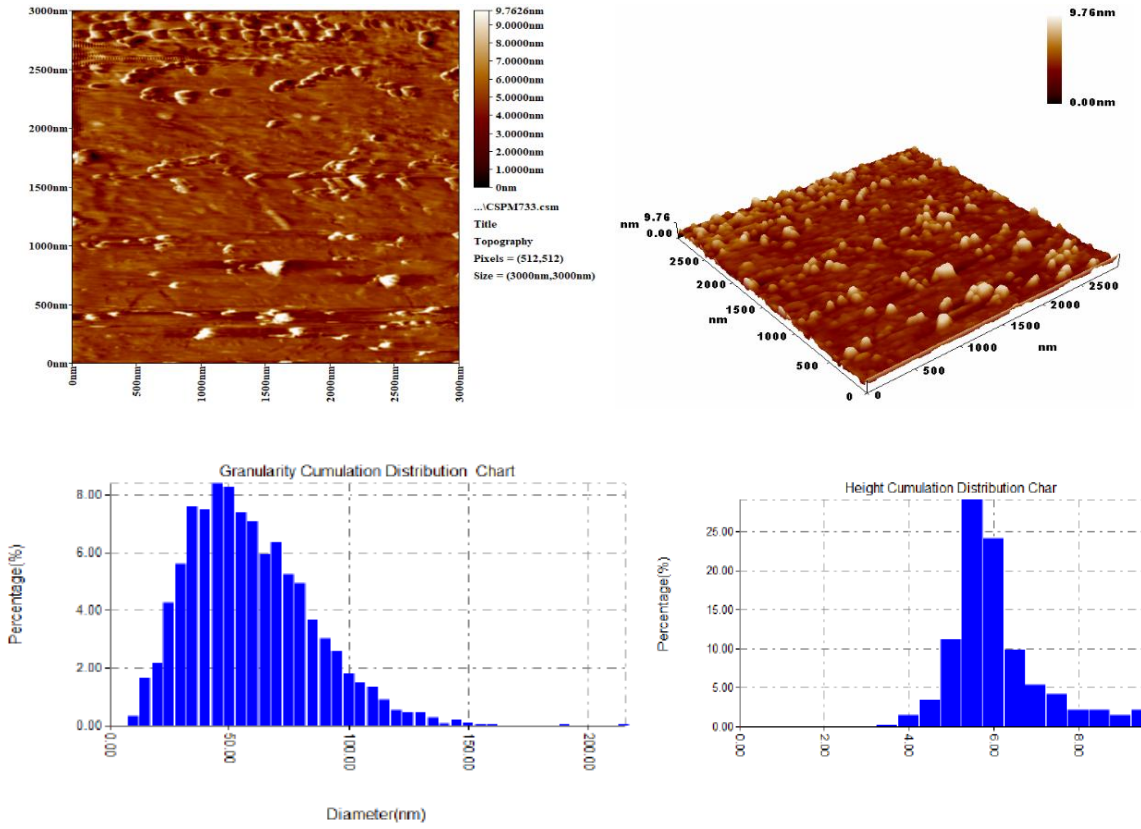

Fig. 7. c. AFM of Au nanofilm layer deposited at 20-second sputtering time

4. Conclusion

DC-sputtering was used to deposit Au nanostructures on quartz substrates for 10, 15, and 20 seconds, and then their characteristics were investigated and studied with UV-Vis, X-ray, and AFM tests. The thicknesses of the three films prepared at different sputtering times were calculated using the empirical formula. A change from blue to green was observed as the sputtering time and the thickness of the gold nanofilms increased, indicating a change in the prepared samples' nanostructure. A non-zero energy gap of gold nanostructure was found by analyzing their UV-Vis spectra using Tauc's model, in which a non-zero band gap indicates semi-conducting properties of the gold-sputtered nanostructures. Results from AFM tests revealed that the surface configuration of the as-sputtered nanostructures does not rely noticeably on the sputter times, where the layered growth stage is related to the monotonic decline of surface roughness with deposition time. Sputtered Au films on quartz substrates revealed a monotonic decline in surface roughness, root-mean-square surface roughness, and grain size as sputtering time was increased. The results revealed that 10 s was the best sputtering time, with the highest roughness and RMS. Gold nanostructures may be evenly and homogeneously distributed on the quartz substrate surface if the experiment is conducted under these conditions. Since the optical properties are dependent on the layer thickness, these ultra-thin films may be used as photocatalyst seed layers in optoelectronic applications. Given that the gold nanoparticles are energetic and productive heat carriers and that the optical properties can be tuned by using various substrate materials like TiO_2, these features could have significant impacts on the development of future solid-state solar cells and chemical gas sensors.

Acknowledgment

The authors would like to express their gratitude to the employees of the Science College, Mustansiriyah University, Technical Engineering College-Baghdad, Middle Technical University for their assistance during this work.

References

[1] R. A. McINTYRE, “Common nano-materials and their use in real world applications,” Sci. Prog., vol. 95, no. 1, pp. 1–22, 2012, doi: doi: 10.3184/003685012X13294715456431.
[2] Z. H. Mohammad, F. Ahmad, S. A. Ibrahim, and S. Zaidi, “Application of nanotechnology in different aspects of the food industry,” Discov. Food, vol. 2, no. 1, p. 12, 2022, doi: https://doi.org/10.1007/s44187-022-00013-9.
[3] I. Khan, K. Saeed, and I. Khan, “Nanoparticles: Properties, applications and toxicities,” Arab. J. Chem., vol. 12, no. 7, pp. 908–931, 2019, doi: https://doi.org/10.1016/j.arabjc.2017.05.011.
[4] A. Axelevitch, B. Apter, and G. Golan, “Simulation and experimental investigation of optical transparency in gold island films,” Opt. Express, vol. 21, no. 4, pp. 4126–4138, 2013, doi: https://doi.org/10.1364/OE.21.004126.
[5] M. Pan et al., “Noble metal nanostructured materials for chemical and biosensing systems,” Nanomaterials, vol. 10, no. 2, p. 209, 2020, doi: https://doi.org/10.3390/nano10020209.
[6] H. Zhong et al., “Thermal-stability resonators for visible light full-spectrum perfect absorbers,” Sol. Energy, vol. 208, pp. 445–450, 2020,

doi: https://doi.org/10.1016/j.solener.2020.08.026.
[7] S. Malik, K. Muhammad, and Y. Waheed, "Nanotechnology: A Revolution in Modern Industry," Molecules, vol. 28, no. 2, p. 661, 2023, doi: https://doi.org/10.3390/molecules28020661.
[8] P. Buffat and J. P. Borel, "Size effect on the melting temperature of gold particles," Phys. Rev. A, vol. 13, no. 6, p. 2287, 1976, doi: https://doi.org/10.1103/PhysRevA.13.2287.
[9] R. S. Sennett and G. D. Scott, "The structure of evaporated metal films and their optical properties," Josa, vol. 40, no. 4, pp. 203–211, 1950, doi: https://doi.org/10.1364/JOSA.40.000203.
[10] F. Gao and Z. Gu, "Melting temperature of metallic nanoparticles," in Handbook of Nanoparticles, Springer, 2016, pp. 661–690. doi: https://doi.org/10.1007/978-3-319-15338-4_6.
[11] C. Kan, X. Zhu, and G. Wang, "Single-crystalline gold microplates: synthesis, characterization, and thermal stability," J. Phys. Chem. B, vol. 110, no. 10, pp. 4651–4656, 2006, doi: https://doi.org/10.1021/jp054800d.
[12] I. Fratoddi et al., "Electronic properties of a functionalized noble metal nanoparticles covalent network," J. Phys. Chem. C, vol. 121, no. 33, pp. 18110–18119, 2017, doi: https://doi.org/10.1021/acs.jpcc.7b07176.
[13] M. Amer and A. J. Ghazai, "Effect of Films Thickness on Structural and Optical Properties of Gold (Au) Thin Films Prepared by DC Magnetron Sputtering," Iraqi J. Sci., pp. 1549–1556, 2022, doi: https://doi.org/10.24996/ijs.2022.63.4.15.
[14] J. C. Maxwell-Garnett, "XII. Colours in metal glasses and in metallic films," Philos. Trans. R. Soc. London. Ser. A, Contain. Pap. a Math. or Phys. Character, vol. 203, no. 359–371, pp. 385–420, 1904, doi: https://doi.org/10.1098/rsta.1904.0024.
[15] M. E. Messing, K. Hillerich, J. Johansson, K. Deppert, and K. A. Dick, "The use of gold for fabrication of nanowire structures," Gold Bull., vol. 42, pp. 172–181, 2009, doi: https://doi.org/10.1007/BF03214931.
[16] M. González-Garnica et al., "One dimensional Au-ZnO hybrid nanostructures based CO2 detection: Growth mechanism and role of the seed layer on sensing performance," Sensors Actuators B Chem., vol. 337, p. 129765, 2021, doi: https://doi.org/10.1016/j.snb.2021.129765.
[17] A. Serrano et al., "Effect of the seed layer on the growth and orientation of the ZnO nanowires: Consequence on structural and optical properties," Vacuum, vol. 146, pp. 509–516, 2017, doi: https://doi.org/10.1016/j.vacuum.2017.03.010.
[18] Y. A. Attia, T. A. Altalhi, and A. A. Gobouri, "Thermal stability and hot carrier dynamics of gold nanoparticles of different shapes," Adv. Nanoparticles, vol. 4, no. 04, p. 85, 2015, doi: 10.4236/anp.2015.44010.
[19] H. B. Liu, J. A. Ascencio, M. Perez-Alvarez, and M. J. Yacaman, "Melting behavior of nanometer sized gold isomers," Surf. Sci., vol. 491, no. 1–2, pp. 88–98, 2001, doi: https://doi.org/10.1016/S0039-6028(01)01351-6.
[20] M. B. Mohamed, Z. L. Wang, and M. A. El-Sayed, "Temperature-dependent size-controlled nucleation and growth of gold nanoclusters," J. Phys. Chem. A, vol. 103, no. 49, pp. 10255–10259, 1999, doi: https://doi.org/10.1021/jp9919720.
[21] F. Liu, P. Rugheimer, E. Mateeva, D. E. Savage, and M. G. Lagally, "Response of a strained semiconductor structure," Nature, vol. 416, no. 6880, p. 498, 2002, doi: https://doi.org/10.1038/416498a.
[22] J. Matovic and Z. Jakšić, "Nanomembrane: A new MEMS/NEMS building block," Micro Electron. Mech. Syst., pp. 61–84, 2009, doi: 10.5772/7004.
[23] A. Curulli, "Nanomaterials in electrochemical sensing area: Applications and challenges in food analysis," Molecules, vol. 25, no. 23, p. 5759, 2020, doi: https://doi.org/10.3390/molecules25235759.
[24] V. Švorčík, O. Kvítek, O. Lyutakov, J. Siegel, and Z. Kolská, "Annealing of sputtered gold nano-structures," Appl. Phys. A, vol. 102, no. 3, pp. 747–751, 2011, doi: https://doi.org/10.1007/s00339-010-5977-5.
[25] Z. I. Ali, S. I. Radwan, M. M. Shehata, O. A. Ghazy, and H. H. Saleh, "Structural, optical and electrical properties of PVC/Au thin films prepared by sputtering process," Opt. Quantum Electron., vol. 53, pp. 1–14, 2021, doi: https://doi.org/10.1007/s11082-021-02876-1.
[26] M. Stoian, T. Maurer, S. Lamri, and I. Fechete, "Techniques of Preparation of Thin Films: Catalytic Combustion," Catalysts, vol. 11, no. 12, p. 1530, 2021, doi: https://doi.org/10.3390/catal11121530.
[27] E. Irissou, B. Le Drogoff, M. Chaker, M. Trudeau, and D. Guay, "Nanostructured gold thin films prepared by pulsed laser deposition," J. Mater. Res., vol. 19, no. 3, pp. 950–958, 2004, doi: https://doi.org/10.1557/jmr.2004.19.3.950.
[28] B. Abbotsford and 33844 King Road Canada, V2S 7M8, Business Center, "Plasma Sputter Coater with Vacuum Pump, MNT-JS1600.,MicroNano Tools/Micromolding Solutions Inc." https://www.micronanotools.com/products/single-target-sputtering-coater-with-vacuum-pump
[29] A. D. Faisal, M. O. Dawood, and K. Hassoon, "Observation of blue shift absorption for surface plasmon resonance in gold nano-islands," Int. J. Nanoelectron. Mater., vol. 12, p. 265, 2019, doi: http://dspace.unimap.edu.my:80/xmlui/handle/123456789/61123.
[30] J. Siegel, O. Lyutakov, V. Rybka, Z. Kolská, and V. Švorčík, "Properties of gold nanostructures sputtered on glass," Nanoscale Res. Lett., vol. 6, pp. 1–9, 2011, doi: https://doi.org/10.1186/1556-276X-6-96.
[31] M. Suchea, S. Christoulakis, K. Moschovis, N. Katsarakis, and G. Kiriakidis, "ZnO transparent thin films for gas sensor applications," Thin Solid Films, vol. 515, no. 2, pp. 551–554, 2006, doi: https://doi.org/10.1016/j.tsf.2005.12.295.
[32] S. H. Sabeeh, "The effects of sputtering time on Cds thin film solar cell deposited by DC plasma sputtering method," Eng. Technol. J., vol. 36, no. 2 Part C, 2018, doi: https://doi.org/10.30684/etj.36.2C.5.
[33] M. Fikry, M. Mohie, M. Gamal, A. Ibrahim, and G. Genidy, "Superior control for physical properties of sputter deposited ITO thin-films proper for some transparent solar applications," Opt. Quantum Electron., vol. 53, pp. 1–16, 2021, doi: https://doi.org/10.1007/s11082-021-02770-w.
[34] H. Stanjek and W. Häusler, "Basics of X-ray Diffraction," Hyperfine Interact., vol. 154, pp. 107–119, 2004, doi: https://doi.org/10.1023/B:HYPE.0000032028.60546.38.
[35] D. D. Le Pevelen, "Small molecule X-ray crystallography, theory and workflow," 2010, https://www.sciencedirect.com/topics/medicine-and-dentistry/braggs-law.
[36] W. Wong-Ng, H. F. McMurdie, C. R. Hubbard, and A. D. Mighell, "JCPDS-ICDD research associateship (cooperative program with NBS/NIST)," J. Res. Natl. Inst. Stand. Technol., vol. 106, no. 6, p. 1013, 2001, doi: 10.6028/jres.106.052.
[37] H. E. Swanson, Standard X-ray diffraction powder patterns, vol. 25. US Department of Commerce, National Bureau of Standards, 1953, [Online] Available: https://books.google.iq/books?hl=en&lr=&id=CtVf1TRPoWcC&oi=fnd&pg=PA2&dq=Swanson,+Howard+Eugene.+Standard+X-ray+diffraction+powder+patterns&ots=8iHhzF5LLL&sig=dqjok9rKZpfD9gqCYMbCC4m-nys&redir_esc=y#v=onepage&q&f=false

[38] A. Monshi, M. R. Foroughi, and M. R. Monshi, "Modified Scherrer equation to estimate more accurately nano-crystallite size using XRD," World J. nano Sci. Eng., vol. 2, no. 3, pp. 154–160, 2012, doi: https://doi:10.4236/wjnse.2012.23020.
[39] Y. Al-Douri et al., "Structural and optical insights to enhance solar cell performance of CdS nanostructures," Energy Convers. Manag., vol. 82, pp. 238–243, 2014, doi: https://doi.org/10.1016/j.enconman.2014.03.020.
[40] M. A. Abdulsattar, "Ab initio large unit cell calculations of the electronic structure of diamond nanocrystals," Solid State Sci., vol. 13, no. 5, pp. 843–849, 2011, doi: https://doi.org/10.1016/j.solidstatesciences.2011.03.009.
[41] M. A. Abdulsattar, "Size variation of infrared vibrational spectra from molecules to hydrogenated diamond nanocrystals: a density functional theory study," Beilstein J. Nanotechnol., vol. 4, no. 1, pp. 262–268, 2013, doi: https://doi.org/10.3762/bjnano.4.28.
[42] V. Švorčík et al., "Annealing of gold nanostructures sputtered on glass substrate," Appl. Phys. A, vol. 102, pp. 605–610, 2011, doi: https://doi.org/10.1007/s00339-010-6167-1.
[43] R. A. Al-wardy and S. K. Rahi, "The Physical Properties and Applications of Gold Nanoparticles (Au NPs)," Samarra J. Pure Appl. Sci., vol. 3, no. 1, pp. 74–86, 2021, doi: https://www.iasj.net/iasj/download/6e8e492168296c75.
[44] J. C. Yannopoulos, "Physical and chemical properties of gold," in The Extractive Metallurgy of Gold, Springer, 1991, pp. 11–23. doi: https://doi.org/10.1007/978-1-4684-8425-0_2.
[45] E. Roduner, "Size matters: why nanomaterials are different," Chem. Soc. Rev., vol. 35, no. 7, pp. 583–592, 2006, doi: https://doi.org/10.1039/B502142C.
[46] V. Svorcık, J. Zehentner, V. Rybka, P. Slepicka, and V. Hnatowicz, "Characterization of thin gold layers on polyethyleneterephthalate: transition from discontinuous to continuous, homogenous layer," Appl. Phys. A, vol. 75, pp. 541–544, 2002, doi: https://doi.org/10.1007/s003390101024.
[47] M. Brust, D. Bethell, C. J. Kiely, and D. J. Schiffrin, "Self-assembled gold nanoparticle thin films with nonmetallic optical and electronic properties," Langmuir, vol. 14, no. 19, pp. 5425–5429, 1998, doi: https://doi.org/10.1021/la980557g.
[48] O. Hunderi, "Optics of rough surfaces, discontinuous films and heterogeneous materials," Surf. Sci., vol. 96, no. 1–3, pp. 1–31, 1980, doi: https://doi.org/10.1016/0039-6028(80)90291-5.
[49] G. Kalyuzhny, A. Vaskevich, M. A. Schneeweiss, and I. Rubinstein, "Transmission surface-plasmon resonance (T-SPR) measurements for monitoring adsorption on ultrathin gold island films," Chem. Eur. J., vol. 8, no. 17, pp. 3849–3857, 2002, doi: https://doi.org/10.1002/1521-3765(20020902)8:17<3849::AID-CHEM3849>3.0.CO;2-1.
[50] S. A. Maier, Plasmonics: fundamentals and applications, vol. 1. Springer, 2007. [Online]. Available: https://link.springer.com/book/10.1007/0-387-37825-1.
[51] S. Link, C. Burda, Z. L. Wang, and M. A. El-Sayed, "Electron dynamics in gold and gold–silver alloy nanoparticles: The influence of a nonequilibrium electron distribution and the size dependence of the electron–phonon relaxation," J. Chem. Phys., vol. 111, no. 3, pp. 1255–1264, 1999, doi: https://doi.org/10.1063/1.479310.
[52] K.-S. Lee and M. A. El-Sayed, "Gold and silver nanoparticles in sensing and imaging: sensitivity of plasmon response to size, shape, and metal composition," J. Phys. Chem. B, vol. 110, no. 39, pp. 19220–19225, 2006, doi: https://doi.org/10.1021/jp062536y.
[53] S. Norrman, T. Andersson, C. G. Granqvist, and O. Hunderi, "Optical properties of discontinuous gold films," Phys. Rev. B, vol. 18, no. 2, p. 674, 1978, doi: https://doi.org/10.1103/PhysRevB.18.674.
[54] V. Amendola, R. Pilot, M. Frasconi, O. M. Maragò, and M. A. Iatì, "Surface plasmon resonance in gold nanoparticles: a review," J. Phys. Condens. Matter, vol. 29, no. 20, p. 203002, 2017, doi: 10.1088/1361-648X/aa60f3.
[55] K. L. Kelly, E. Coronado, L. L. Zhao, and G. C. Schatz, "The optical properties of metal nanoparticles: the influence of size, shape, and dielectric environment," The Journal of Physical Chemistry B, vol. 107, no. 3. ACS Publications, pp. 668–677, 2003. doi: https://doi.org/10.1021/jp026731y.
[56] I. Doron-Mor, Z. Barkay, N. Filip-Granit, A. Vaskevich, and I. Rubinstein, "Ultrathin gold island films on silanized glass. Morphology and optical properties," Chem. Mater., vol. 16, no. 18, pp. 3476–3483, 2004, doi: https://doi.org/10.1021/cm049605a.
[57] R. H. Doremus, "Optical properties of thin metallic films in island form," J. Appl. Phys., vol. 37, no. 7, pp. 2775–2781, 1966, doi: https://doi.org/10.1063/1.1782121.